PERCOLATION ON UNIFORM INFINITE TRIANGULATIONS

YUYANG FENG

Abstract. We will introduce the uniform infinite planar triangulations (UIPT) and uniform infinite half-plane triangulations (UIHPT). Then we will study Bernoulli site percolation on UIHPT using a method different from the literature, and explain that a.s. the critical probability $p_c = 1/2$. Moreover, in the sub-critical region, the size of the whole cluster will have a polynomial decay, and in the super-critical region, there will a.s. exist a unique infinite cluster.

Contents

1. Introduction

In the past few decades, there have been plenty of works concerning random planar maps. A random planar map is a graph embedded into the Riemann surface with genus 0 in a way that no two edges cross, viewed modulo orientation-preserving homeomorphism. The study of planar maps dates back to the 1960s with Tutte's attempts at the four-color problem. There are some combinatorial results about counting a class of maps in his series of papers [41] [39] [42] [40].

One of the motivations for studying planar maps comes from statistical mechanics. The planar maps are discrete analogs of LQG (Liouville quantum gravity) surfaces, which are random topological surfaces equipped with a measure, a metric, and a conformal structure. It plays a vital role in many physics models which tracked back to the foundational work of Polyakov [33]. The earliest mathematical studies include [34] and [16]. The idea of the latter is to consider the surface with volume measure $e^{\gamma h} d^2 z$. Here, h is a generalized function called GFF (Gaussian

Date: January 12, 2022.

free field), and γ is a parameter. For more background on LQG, we recommend the lecture notes [7] and the survey paper [19].

Uniform random planar maps are the simplest and the most natural planar map models, corresponding to the "pure gravity" in physics. We can prove the existence of the weak limit of uniform measure on finite triangulations with respect to the local metric, a sample of which is called UIPT (uniform infinite planar triangulation). UIPT was first suggested in [6], a primary goal of which is to understand the large-scale geometry. And the existence was first proved by Angel and Schramm in [5]. We can also define UIPQ for quadrangulation (established in [24]) and UIHPT for half-plane (established in [2]).

We remark that, in addition to local limits, one can also consider scaling limits of uniform random planar maps in the Gromov-Hausdorff topology. The scaling limit of the uniform planar map of the sphere is the Brownian sphere [27] [30]. Furthermore, the Brownian sphere is equivalent to LQG with parameter $\gamma = \sqrt{8/3}$, proved by Miller and Sheffield [31] [32]. There is a vast literature and we will not cover the scaling limits in this paper.

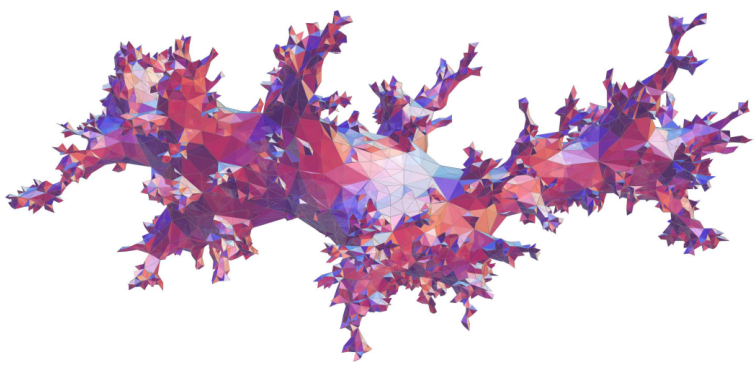

FIGURE 1.1. A simulation of uniform triangulation with 10000 triangles embedded in $\mathbb{R}^3$ by Curien [13]

A significant tool to study uniform planar maps is peeling. Roughly speaking, peeling is a process in which we explore the map one face at a time, like peeling an apple. It was first suggested in the physics literature by Watabiki [43] without a precise justification. Angel first defined it rigorously and used it to study percolation on UIPT [1]. To deal with maps with more general boundaries, Budd introduced lazy peeling to make a unified treatment [10]. There have been many results proven using peeling, but we will not mention them in this paper except site percolation on UIHPT.

Bernoulli (site) percolation with parameter $p \in [0, 1]$ is a model that each vertex independently has probability p to be open and $1 - p$ to be closed. We recommend [44] for more background. Instead of fixed lattice, one can also ask questions for percolation in random planar maps. To our knowledge, Kazakov first did such research in [22] about bond percolation on random triangulations while not rigorously. The first mathematical work is due to Angel [1] using peeling to prove the

threshold for site percolation on UIPT is a.s. 1/2. Angel and Curien extended these results for bond and face percolation on UIHPT and UIHPQ in [3]. The result for site percolation on quadrangulations is later proved by Richier [35].

One can also consider the scaling limits of percolation interfaces on random planar maps, the candidates of which are SLE_κ. Here, SLE_κ (Schramm-Loewner evolution) is a family of random curves with fractal structures introduced by Schramm [36]. SLE have deep relationship with LQG [15] [37]. Recall LQG surface is expected to be the scaling limit of random planar map, thus it is natural to find a corresponding object of SLE in random planar maps. Aizenman conjectures the scaling limits of the percolation interfaces are conformally invariant [25], which is the property of SLE. For this reason, people believe interfaces for critical percolation on various deterministic lattices will converge to SLE_6. We choose SLE_6 as the limit since it is the only candidate with locality property [26]. This was proven by Smirnov for site percolation on the triangular lattice [38], but remains open for other percolation models on other deterministic lattices. Similarly, critical percolation interfaces on random planar maps converge to SLE_6 on LQG surfaces. There are several subtleties in this statement, including the topology of convergence and how to even define SLE_6 on an LQG surface. We will not discuss these subtleties here. Instead, we refer to [20][21] for scaling limit results for percolation on uniform random planar maps toward SLE_6. Here, peeling plays a major role in the proof of the convergence.

The paper is organized as follows. In section 2, we present the definition of UIPT and UIHPT from three different points of view: as a uniform measure, which is the original definition; as a Markov process, where peeling is used to give another sampling way; and as a random tree. In section 3, we study percolation on UIHPT (the method is also suitable for UIPT). The author proves the following theorem using a different way from previous literature, and as a by-product, the cluster size's polynomial decay in the sub-critical region.

Theorem 1.1. *In site percolation on UIHPT with free boundary condition, let k_p denote the number of infinite clusters. Then $k_p = 0$ a.s. for $p \leq \frac{1}{2}$; $k_p = 1$ a.s. for $p > \frac{1}{2}$.*

The main references for this paper are [5], which proves the existence of UIPT; [1], which introduces peeling; [3], which studies percolation on uniform UIHPT. We also recommend [13] as an expository note with more general results and many open questions.

The author finished this paper during the REU project in the University of Chicago, mentored by Prof. Ewain Gwynne. The author is supported by the Elite Undergraduate Training Program of the School of Mathematical Sciences at Peking University.

2. UIPT

2.1. **Definitions.** A planar map is an embedded graph viewed modulo orientation-preserving homeomorphisms. Thus besides linking relations in the underlying graph, we do have a topology structure here. Furthermore, we can also define a metric in the space of planar maps, which will be given later. Therefore, the statement of convergence will make sense.

By conventions, we only consider the locally finite graphs in this paper, i.e., each vertex has a finite degree. All the graphs we discuss in this paper will be 2-connected (i.e. allow multiple edges, but self-loops are not allowed.) We can also consider the class of 1-connected maps that allow self-loops. There will be similar results but perhaps different parameter values.

Definition 2.1. A root in a planar map $\mathbf{m}$ is a unique face f with an oriented edge $\overrightarrow{xy}$ on the boundary of f. We call x the root vertex (or origin) and $\overrightarrow{xy}$ the root edge. We identify two rooted triangulations if there is an orientation-preserving homeomorphism mapping the root to root.

Rooting is a tool to kill the symmetries for the convenience of counting. It comes from the fact that an automorphism fixing an oriented edge will fix all the oriented edges [28, Proposition 5.1]. Thus the only automorphism of a rooted map is identity.

Let R-ball (or B_R) be the submap formed by the vertices and edges at graph distance $\leq R$ from the origin. Then we can define a local metric (following [6]) in the space of planar graphs as below. It's easy to check that it is well-defined, with those R-balls as a topology basis.

Definition 2.2 (Local metric)**.** For two rooted map $\mathbf{m}, \mathbf{m}'$,

$$\mathrm{d}_{\mathrm{loc}}(\mathbf{m}, \mathbf{m}') := (1+R)^{-1}$$

where R is the maximal radius such that R-balls of $\mathbf{m}$ and $\mathbf{m}'$ are homeomorphic while preserving oriention.

We call a planar map a triangulation if all of its faces are triangles. We will mainly consider rooted triangulations of the sphere and denote the space of all such rooted maps by $\mathcal{T}$. We endow $\mathcal{T}$ with the local metric.

Proposition 2.3. $\mathrm{d}_{\mathrm{loc}}$ *in* $\mathcal{T}$ *is complete.*

Proof. Given a Cauchy sequence $\{T_n\}$ for $\mathrm{d}_{\mathrm{loc}}$, then for any R, there is a N such that all $n_1, n_2 > N$, $\mathrm{d}_{\mathrm{loc}}(T_{n_1}, T_{n_2}) < (1+R)^{-1}$. Hence, T_n will agree on the R-ball for all $n > N$. We construct the T s.t. $B_R(T)$ is this common R-ball. T is well-defined since there is a relationship of inclusion between these R-balls. Moreover, $T \in \mathcal{T}$, and $\mathrm{d}_{\mathrm{loc}}(T, T_n) \to 0$. □

Furthermore, we can consider triangulations with simple boundaries, or in other words, triangulations of the polygon. For the sake of simplicity, we denote a polygon of length m by m-gon. Let $\mathcal{T}_m$ be the set of rooted triangulations of m-gon with a specifically directed root edge in the boundary.

Proposition 2.4. $\mathcal{T}_m \overset{1:1}{\longleftrightarrow} \{\mathbf{m} \mid \mathbf{m} \hookrightarrow \mathbf{S}^2$*, with all faces triangles except a* m*-gon root.*$\}$*. Specifically,* $\mathcal{T}_3$ *is equivalent to* $\mathcal{T}$*.*

Proof. When we add a m-gon face of $T \in \mathcal{T}_m$, we get an embedded planar map on the right set, where the root is the added face, and the root edge is the original one. When we remove the m-gon root of an element on the right side, we get a triangulation of m-gon and the original root edge as the new root edge. This correspondence is well-defined for the equivalence relationship. Here we get the bijection. □

We can also define p-gulation as the planar map where all faces are p-gons. More generally, if we imagine gluing faces to get the planar maps like putting the jigsaw pieces together, we can also define a weight sequence $\mathbf{q}$ of the different pieces. When $\mathbf{q}$ is "admissible" [13], we can conclude similar things that we will discuss in this paper. Readers with interests can read the lecture notes [13] for more details.

For terminology we will use later, if T is a triangulation of a region of the sphere (maybe with some holes), we call these holes external faces, and edges (resp. vertices) on its boundary external edges (resp. vertices). For the remaining edges (resp. vertices) of T, we call them internal edges (resp. vertices). We will denote the number of internal vertices by $|T|$.

2.2. **UIPT as uniform measure.** When we want to give a distribution in $\mathcal{T}$, one natural idea is to give a "uniform" measure. Combinatorial counting techniques from Tutte [41] provide us a vehicle to define the uniform measure of finite triangulations.

Proposition 2.5 (Tutte's formula [18])**.** *Let $\varphi_{n,m}$ denote the number of triangulations $T \in \mathcal{T}_m$, $|T| = n$. For $n \geq 0$, $m \geq 2$,*

$$\varphi_{n,m} = \frac{2^{n+1}(2m-3)!(2m+3n-4)!}{(m-2)!^2 n!(2m+2n-2)!}$$

For the sake of convenience, we use Stirling's formula to get the asymptotics:

$$\varphi_{n,m} \sim C_m \alpha^n n^{-\frac{5}{2}}, n \to \infty \tag{2.1}$$

$$C_m \asymp \beta^m \sqrt{m}, m \to \infty. \tag{2.2}$$

In our case of 2-connected triangulations, $\alpha = 27/2, \beta = 9$. For 1-connected triangulations and quadrangulations, readers can look up [3, §2.2] and its references. A general Tutte's formula can be found in [13, §3]. Using the above result and Propositon 2.4, we know exactly the number of n vertices triangulation of the sphere, which is $\varphi_{n-3,3}$.

Definition 2.6. τ_n is the uniform distribution on triangulations of the sphere with n vertices.

Theorem 2.7 ([5])**.** *There exists a distribution τ on $\mathcal{T}$ s.t. $\tau_n \xrightarrow{d} \tau$ with respect to $\mathrm{d_{loc}}$.*

It was first proved by Angel and Schramm in [5]. The idea is to show the tightness first. Then any subsequence will have further subsequence that is convergent. Second, we show that if a subsequence has a limit, then the limit is unique (by some characteristic properties we get for a limit). Thus by an ordinary argument (see [17, §3.2] for example), we get our proposition.

Definition 2.8. A sample of τ is called UIPT (uniform infinite planar triangulation).

Remark 2.9. Replacing the triangle root by m-gon, we can use a similar technique in Theorem 2.7 to prove the weak convergence of uniform measure of m-gon. We denote the weak limit by τ^m and the sample by UIPT of m-gon.

It is easy to see τ (resp. τ^m) is supported on infinite triangulations $\subset \mathcal{T}$ (resp. $\mathcal{T}_m$). The word "planar" in the name comes from the following observation, proved in [5, §3.2]:

Proposition 2.10 ([5]). *We call a graph G one-ended if for any subgraph H, $G \setminus H$ has exactly one infinite connected component. Then, UIPT (of m-gon) is a.s. one-ended.*

Regarding the finite triangulations of m-gon, it is natural to give a partition function such that $|T| = n$ with weight θ^n for some $\theta > 0$. Then the total mass is $Z_m(\theta) = \sum_{n=0}^{\infty} \varphi_{n,m}\theta^n$. One can check $\theta = \alpha^{-1}$ is the critical value for $Z_m(\theta)$ to be infinite or decays exponentially [18]. Let $Z_m(\alpha^{-1}) = Z_m$ for simplicity.

Definition 2.11 (Boltzmann distribution of a m-gon). When $T \in \mathcal{T}_m$, $|T| = n$,

$$\mu_m(T) := \frac{\alpha^{-n}}{Z_m}$$

In the following, we say a sample T contains a rooted submap A, or $A \subset T$, if A appears in T with coinciding roots.

Definition 2.12. We call a rooted submap A rigid if it is:
(1) finite. (2) connected. (3) any $T \in \mathcal{T}$ can't contain two distinct copies of A.

For example, R-balls are rigid. With the definition, triangulations containing A are in bijection with the ways of filling the holes of A with triangles.

Proposition 2.13. *Let A be rigid and with k external faces of length $m_1, \ldots, m_k$. Let $R_i = R_i(A)$ denote the event "$A \subset T$, all external faces have finitely many vertices except the i'th one". For a UIPT containing A, let T_j be the component of the j-th face. Then condition on $R_i(A)$, the followings hold:*

1. These T_j are independent.
2. $T_i \overset{d}{=}$ UIPT of m_i-gon, i.e. follows τ^{m_i}.
3. $T_j \overset{d}{=}$ Boltzmann triangulation of m_j-gon, i.e. follows μ_{m_j}, for $j \neq i$.

Proof. We may asume $i = 1$. Let $T(n_2, \ldots, n_k)$ denote the event "$A \subset T$ and $|T_j| = n_j$ $(j > 1)$". Let n be the number of vertices in A and its boundary. Thus for $N > n + n_2 + \ldots n_k$, let $n_1 = N - n - n_2 \cdots - n_k$, then:

$$\begin{aligned}
\lim_{N\to\infty} \tau_N(T(n_2, \ldots, n_k)) &= \left(\prod_{i>1} \varphi_{n_i,m_i}\right) \lim_{N\to\infty} \frac{\varphi_{n_1,m_1}}{\varphi_{N-3,3}} \\
&= \left(\prod_{i>1} \varphi_{n_i,m_i}\right) \lim_{N\to\infty} \frac{C_{m_1} n_1^{-5/2} \alpha^{n_1}}{C_3 (N-3)^{-5/2} \alpha^{N-3}} \\
&= \left(\prod_{i>1} \varphi_{n_i,m_i} \alpha^{-n_i}\right) \frac{C_{m_1} \alpha^{3-n}}{C_3}
\end{aligned}$$

The second equation comes from (2.1). Sum all possible $(n_2, \ldots, n_k)$, we can get:

$$\tau(R_1) = \frac{C_{m_1} \alpha^{3-n}}{C_3} \prod_{i>1} Z_{m_i}$$

Thus the conditional law is given by:

$$\tau(|T_j| = n_j,\ j > 1 \ |R_1) = \prod_{i>1} \frac{\varphi_{n_i,m_i} \alpha^{-n_i}}{Z_{m_i}} \tag{2.3}$$

From the product representation, we see T_j are independent from each other. Furthermore, for any $(n_2, \ldots, n_k)$, $\tau_N(\cdot \mid T(n_2, \ldots, n_k))$ is uniformly distributed in $\{T \in \mathcal{T}_{m_1} \mid |T| = n_1\}$. Thus it tends to UIPT of m_1-gon and independent of $T_2, \ldots, T_k$. □

Now we introduce our protagonist in Chapter 3. A sample of the weak limit is called UIHPT (uniform infinite half-plane triangulation) since you can imagine as the length of boundary tends to infinity, the graph will tend to a one-ended disk, which can be regarded as a triangulation of the half-plane.

Proposition 2.14 ([2])**.** *There exists a distribution τ^∞ on $\mathcal{T}$ s.t. $\tau^m \xrightarrow{d} \tau^\infty$, with respect to $\mathrm{d}_{\mathrm{loc}}$.*

The existence is proved in [2] and we use $\mathbf{M}$ to represent UIHPT following the notation in [3]. We define a shift operator θ s.t $\theta\mathbf{M}$ is the map obtained by re-rooting $\mathbf{M}$ a boundary edge in the immediate left to the original one.

Lemma 2.15. $\theta\mathbf{M} \overset{d}{=} \mathbf{M}$

Proof. For UIPT of m-gon, re-rooting gives a bijection hence preserves the distribution. Taking the limit, we know it is also true for UIHPT. □

Thus the root edge is not important in UIHPT. We will often omit the root in the following context or just use "root edge" to represent some specific edges on the boundary. UIHPT has great spatial Markov property, which we will discuss later.

2.3. **UIPT as Markov process.** Suppose we have explored a finite region of UIPT. We want to find the conditional law of the next step in the external faces. From Theorem 2.13 we know when conditioned on the boundary length m, it is equivalent to consider either Boltzmann triangulation or UIPT of m-gon.
Case 1. (Boltzmann triangulation of m-gon.)

Let $x_1, \ldots, x_m$ be the boundary vertices, with root edge $x_m x_1$. Consider a new triangle growing from the root edge $x_m x_1$. There are two cases:

(1) The third vertex y is internal.

Fix y, the remaining part is $m+1$-gon. Note if there is n vertices in this part, we have $n+1$ vertices in original region. We get the total weight of this situation is

$$\sum\nolimits_{n=0}^{\infty} \varphi_{n,m+1} \alpha^{-n-1} = \alpha^{-1} Z_{m+1}$$

Whence the Boltzmann law (recall μ_m represent Boltzmann triangulation of m-gon):

$$\mu_m(y \text{ is internal}) = \frac{Z_{m+1}}{\alpha Z_m} \tag{2.4}$$

(2) $y = x_i$ in the boundary.

Then the triangle divides m-gon into two regions: an i-gon and a $m-i+1$-gon. Consider all possibilities of respectly (n_1, n_2) vertices in each region, we get total mass:

$$\sum_{n_1, n_2} \varphi_{i,n_1} \varphi_{m-i+1,n_2} \alpha^{-n_1-n_2} = Z_i Z_{m-i+1}$$

Whence the Boltzmann law:

$$\mu_m(y = x_i) = \frac{Z_i Z_{m-i+1}}{Z_m} \tag{2.5}$$

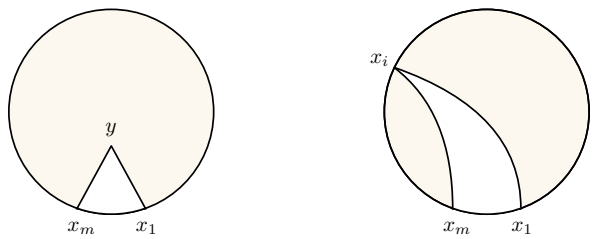

FIGURE 2.1. Left is case (1). Right is case (2). Yellow regions are the unexplored parts.

Case 2. (UIPT of m-gon.)

Let $x_1, \ldots, x_m$ be the boundary vertices, with root edge $x_m x_1$. Consider a new triangle growing from the root edge $x_m x_1$. There are two cases:

(1) The third vertex y is internal.

Fix y, the remaining part is $m+1$-gon, and note if there are n vertices in this part, we have $n+1$ vertices in the original region. (Recall τ^m represent UIPT of m-gon):

$$\tau^m(y \text{ is internal}) = \lim_{N\to\infty} \frac{\varphi_{m+1,N-1}}{\varphi_{m,N}} \overset{(2.1)}{=} \frac{C_{m+1}}{\alpha C_m} \tag{2.6}$$

(2) $y = x_i$ in the boundary.

Let T_1 denote the triangulation in region enclosed by $x_1, \ldots, x_i$, and T_2 the other part. Then by one-endness exactly one of them is infinite. When $T \in \mathcal{T}_i, |T| = n < \infty$,

$$\tau^m(y = x_i, T_1 = T) = \lim_{N\to\infty} \frac{\varphi_{N-n,m-i+1}}{\varphi_{N,m}} = \frac{C_{m-i+1}\alpha^{-n}}{C_m}$$

Thus sum all possible finite T:

$$\tau^m(y = x_i, T_1 \text{ is finite}) = \sum_{n=0}^{\infty} \varphi_{n,i}\alpha^{-n}\frac{C_{m-i+1}}{C_m} = \frac{Z_i C_{m-i+1}}{C_m} \tag{2.7}$$

Similarly, for finite T_2 :

$$\tau^m(y = x_i, T_2 \text{ is finite}) = \sum_{n=0}^{\infty} \varphi_{n,m-i+1}\alpha^{-n}\frac{C_i}{C_m} = \frac{Z_{m-i+1} C_i}{C_m} \tag{2.8}$$

Remark 2.16. From the above, we can see the conditional law only depends on the boundary length of the revealed region, which implies the Markov property.

Theorem 2.17. We can sample UIPT in the following way:

(1) Start from the root edge. The infinite external face at this moment can be regarded as a hole of length 2.

(2) Grow a new triangle from a specific edge on the boundary of current infinite external face. The location of the third vertex and the new infinite external face follow laws (2.7) (2.8) (2.6). The choice of the edge follows some algorithm that is independent of the unrevealed part.

(3) When a finite hole is formed, we fill it with Boltzmann triangulation.

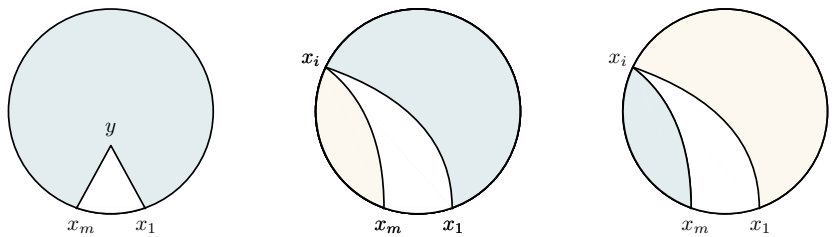

FIGURE 2.2. Left is case (1). Middle and right is case (2), respectively T_1 and T_2 are infinite. We use blue to represent the infinite part and yellow to the finite part.

This process is called peeling, and it is Markovian by Remark 2.16. Peeling was first introduced by Watabiki in [43] while Angel first studied it rigorously in [1]. We use the name peeling as you can imagine we explore the plane like peeling an apple piece by piece. Peeling is a useful tool to study planar maps since it translates two-dimensional problems into one-dimensional Markov processes.

There is much freedom for us to choose the algorithm in step (2). For example, we can explore the edge clockwisely in the boundary until all the adjacent triangles of the old edges have been explored. This will ensure we reveal the r-ball neighborhood of the origin completely before proceeding to $r+1$-ball.

The process is well-defined since the graph is a.s. locally finite [5]. Thus r-balls are a.s. finite, and each stage will be a.s. finished within finite steps. From the local topology, we know these r-balls determine UIPT. Hence this process indeed gives a sample of UIPT.

When we turn our sight into the UIHPT (denote a sample by $\mathbf{M}$), the Markov property becomes stronger. Recall that the one-step distribution in the plane only depends on the length of the boundary, the half-plane no longer be limited to this since we have taken length of the boundary to infinity.

We say a measure on the half-plane is spatial Markov if excluding any finite domain (simply connected) adjacent to the boundary, the new graph we get is in the same distribution to the original one and independent of this finite domain.

Proposition 2.18. *UIHPT is spatial Markov.*

Proof. When peeling a new triangle from an edge on $\partial(\mathbf{M}\setminus D)$, there are two cases: (1) The third vertex y is in the interior. We denote the probability by q_{-1}. (2) The third vertex y is on the boundary. We let q_k be the probability of y at distance k to the left of the peeling edge (the right case by symmetry). Thus by (2.6) and (2.7),

$$q_{-1} = \lim_{m\to\infty} \frac{C_{m+1}}{\alpha C_m} = \frac{\beta}{\alpha} = \frac{2}{3} \tag{2.9}$$

$$q_k = \lim_{m\to\infty} \frac{Z_{k+1}C_{m-k}}{C_m} = Z_{k+1}\beta^{-k} \tag{2.10}$$

These probabilities do not rely on D, and we have a stable next-step law during the process. We will give a peeling process of UIHPT. Using a similar algorithm for UIPT, we know this process also determines UIHPT. Thus the stability of the next-step law tells us the spatial Markov property. □

Definition 2.19. A peeling process is a random algorithm to explore the triangulations in the half-plane. Let $\mathbf{M}_i$ denote the configuration after i-th step:

(1) We start the process from $\mathbf{M}_0 = \mathbf{M}$ and let a_1 be the root edge.

(2) In step i, we choose a peeling edge a_i in $\partial\mathbf{M}_{i-1}$ following the algorithm. The choice of a_i is independent of the unrevealed part.

(3) $\mathbf{M}_i$ is obtained by removing from $\mathbf{M}_{i-1}$ the triangle adjacent to a_i along with the finite region it enclosed.

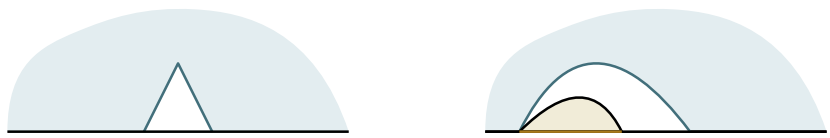

FIGURE 2.3. Cases of one-step peeling. The exposed edges are in blue and the swallowed edges are in yellow. Blue region are the configuration after one-step peeling. Yellow region is the finite hole.

The edges of the newly peeled triangle that become part of the new boundary are called exposed. The edges in an old boundary that the peeled triangle has enclosed are called swallowed (See Figure 2.3. Let $\mathcal{E}$ and $\mathcal{R}$ (resp. $\mathcal{L}$) denote the number of exposed edges and swallowed edges on the right (resp. left) of the peeling edge. Then the above proposition is equivalent to saying that:

$$\tau^{\infty}((\mathcal{E},\mathcal{R}) = (e,r)) = \begin{cases} q_{-1} & (e,r) = (2,0) \\ q_k & (e,r) = (1,k), k > 0. \end{cases} \tag{2.11}$$

Proposition 2.20. *Let $\delta = \mathbb{E}(\#$ swallowed edges$)$. Then:*

$$\mathbb{E}(\mathcal{E}) = 1 + \delta \quad \textit{and} \quad \mathbb{E}(\mathcal{R}) = \mathbb{E}(\mathcal{L}) = \frac{\delta}{2} \tag{2.12}$$

Proof. $\mathcal{R} \overset{d}{=} \mathcal{L}$ by symmetry, thus we get the equation on the right. For $\mathbb{E}(\mathcal{E})$, it could be computed directly. We can also use the spatial Markov property, which implies $0 = \mathbb{E}(\mathcal{E} - \mathcal{R} - \mathcal{L} - 1)$. Here, minus 1 is due to the peeling edge. □

The parameter δ plays a key role in determining thresholds in various planar map models. In our case $\delta = \frac{2}{3}$. For more cases, the readers can look up [3, §2.3].

Theorem 2.21. Let P_i denote the visited parts as well as the finite region it enclosed before step i. Then:

1. $\mathbf{M}_i \overset{d}{=} \mathbf{M}$ and independent of P_i.
2. $(\mathcal{E}_i, \mathcal{R}_i)$ is an i.i.d. sequence with distribution in (2.11) and mean in (2.12).

Proof. We prove it by induction. The first step follows from our previous discussions. When it holds for first i steps, we have $\mathbf{M}_i \overset{d}{=} \mathbf{M}$. Since a_i is independent of $\mathbf{M}_i$, it is also in distribution of $\mathbf{M}$ when we reset a_i as its root edge (by Lemma 2.15). Similar to step 1, we prove the argument about distribution. The argument of independence comes from the spatial Markov property. □

Corollary 2.22. *(Strong Markov property) For a finite stopping time $\mathcal{N}$, $\mathbf{M}_{\mathcal{N}}$ is independent of $P_{\mathcal{N}}$ and in the law of UIHPT.*

We can also estimate the area and the boundary length of the peeling clusters. Readers with interests can see Angel's paper [1] and Curien's lecture notes [13].

2.4. **UIPT as random trees.** We consider the layer of triangles at distance between r and $r+1$ from the origin. First, the number should be a.s. finite. Second, we can draw a new tree with vertices in r-level corresponding the external faces in B_r. The linking relation is given by: suppose there is k_r external faces $x_{1,r}, \ldots, x_{k_r,r}$ in B_r, then this layer may fill or divide some faces. Let $x_{1,r+1}, \ldots, x_{k_{r+1},r+1}$ be the new external faces in B_{r+1}. If $x_{j,r+1} \subset x_{j',r}$, we draw a line between the two faces (regarded as nodes). Note any node only has one parent, it is indeed a tree. Furthermore, we label each node in the tree with the corresponding boundary length of the outer face (see Figure 2.4).

We have the following observations:

1. An infinite triangulation corresponds to an infinite tree.
2. Condition on the r-th level of the tree, the remaining sub-trees are independent by Markov property. Especially, the tree obtained from UIHPT has a fractal structure.
3. Almost all trees have only one infinite branch, carrying many finite sub-trees. This is due to one-endlessness.

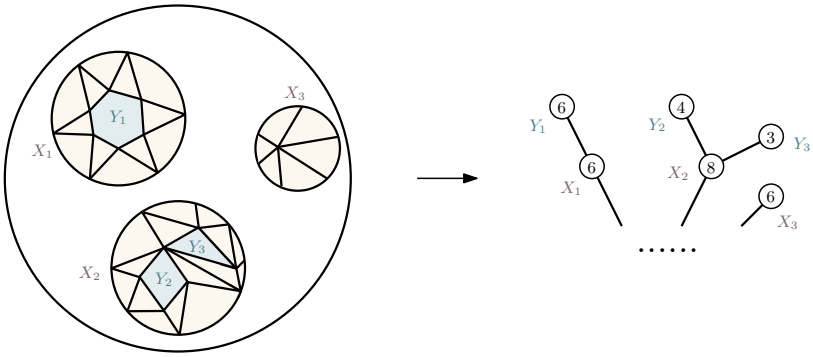

FIGURE 2.4. Tree-like structure. The nodes in the tree are labeled with the boundary length.

In fact, this process is a multi-type GW process conditioned to survive. We can also construct a GW process by this way, see [29]. As an application, we can get a functional invariance principle, where the limiting process is described by a self-similar growth-fragmentation process. The interested reader can consult [9] for further result.

3. PERCOLATION

We have known fruitful results about Bernoulli percolation in the deterministic lattice, which can be found in introductory lecture notes such as [44]. Here, Bernoulli (site) percolation with parameter $p \in [0, 1]$ on a given graph is a model that each vertex independently has probability p to be white and probability $1 - p$ to be black. When there is an infinite white cluster, we say the graph percolates. A natural question is finding values of p such that we have positive probability to percolate.

We can also ask questions about percolation in random environments. Are there similar results? How many environments have positive probabilities to hold this property? We will investigate some analogous properties in this section. In fact, we can regard percolation in the planar map as some "decorated" process. To avoid confusion, we use $\mathbb{P}_p$ to represent the product measure of the planar map (we will mostly discuss UIHPT) and the Bernoulli-p percolation it carries.

Before we start, there is some terminology need to be reviewed. For a random environment in law of μ, and $\mathbb{P}$ as the product measure of its decorated process, the annealed probability of an event E is $\mathbb{P}(E)$ and the quenched probability is $\mathbb{P}(E \mid T)$, where T is a sample of μ.

An example is the threshold of the percolation in UIHPT (in law of τ^∞). In deterministic lattice, p_c is called threshold if any $p > p_c$, it will have positive probability percolate; whilst for $p < p_c$, it cannot percolate in a.s sense. Thus, we say p_c is the annealed threshold if

$$p_c = \inf_p \mathbb{P}_p(T \text{ percolate}) > 0.$$

We say p_c is the quenched threshold if

$$p_c = \inf_p \mathbb{P}_p(\text{percolate} \mid T) > 0, \text{ for a.s. } T.$$

We will prove the annealed threshold for site percolation on UIHPT is $1/2$. Then, we will show it is also quenched threshold by $0-1$ law. The annealed and quenched threshold for site percolation on UIPT are also $1/2$, which can be found in [1, §7]. Bond and face percolation can be found in [3, §3]. They can be proved via similar method in Theorem 3.1, of which the key idea is peeling. It is also worth mentioning that when we think about the threshold p_c' for the dual graph, a fact is that $p_c + p_c' = 1$. The proof of this unsurprising fact can also be found in [3].

3.1. **The thresholds.** To make things easier, We first begin to study the percolation with special boundary conditions: the origin is white, and other vertices in the boundary are black. Despite the boundary, other vertices obey independent Bernoulli percolation: probability p to be white, $1-p$ to be black.

Proposition 3.1. *The annealed threshold for full black boundary except the root vertex is* $\frac{1}{2}$.

Proof. We first define the peeling algorithm:

Boundary condition: Black-white-black: $\cdots - \bullet - \circ - \cdots - \circ - \bullet - \ldots$

Algorithm: We always peel from edge $a_{i-1} : \bullet - \circ$ in $\partial \mathbf{M}_{i-1}$ as long as such edge exists. If the third vertex is inside $\mathbf{M}_{i-1}$, we reveal its color.

Terminate: If there is no white vertex in the boundary.

From Figure 3.1 we can see boundary condition is maintained during the process. The algorithm is well-defined and indeed a peeling process. This is because before termination we will have a unique a_i to peel by the boundary condition. Moreover, the selection of a_i is independent of the unrevealed part.

Lemma 3.2. *For a.s. T, the origin is in infinite white cluster $\Leftrightarrow$ the process never terminate.*

Proof. When terminated, the root vertex will be surrounded by black vertices, and the white cluster will be limited in this finite region, which implies a finite number of white vertices.

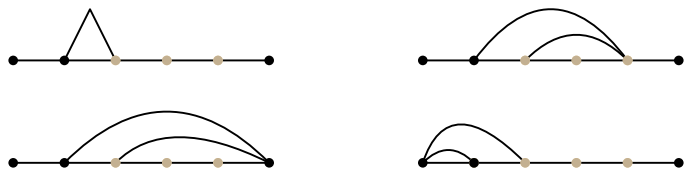

FIGURE 3.1. Different cases when peeling on site percolation configuration.

Note white vertices on the boundary are "continuous" i.e. can be connected in a white path to the root. If the process never terminate while the cluster has a finite size, there will be N such that the number of white vertices in boundary $< N$ at any time. However $q_N > 0$ (2.10), thus a.s. the white vertices in the boundary will be swallowed at some time $\Rightarrow$ a.s. terminate, a contradiction. $\square$

Return to our proof. Let $W_i :=$ the number of white vertices on $\partial \mathbf{M}_i$. Thus $W_0 = 1$. Let $\epsilon_n = 1$ if in step n, a new white vertex is revealed; $\epsilon_n = 0$ otherwise. Thus we have:

$$W_n = (W_{n-1} + \epsilon_n - 1\{\mathcal{R}_n > 0\}\mathcal{R}_n)^+$$

Let the stopping time $\mathcal{N}^-$ be the first time that W_i hits $\mathbb{Z}^- = \{0, -1, -2, \dots\}$. Before $\mathcal{N}^-$, $\{W_n\}$ is a sequence with i.i.d increments (recall Theorem 2.21):

$$X_n = \epsilon_n - 1\{\mathcal{R}_n > 0\}\mathcal{R}_n$$

We have $\mathbb{E}(X_n) = p\mathbb{E}(\mathcal{E} - 1) - \mathbb{E}(\mathcal{R}) \overset{(2.12)}{=} \delta(p - \frac{1}{2})$. Thus when $p \leq \frac{1}{2}$, $\mathbb{E}(X_n) \leq 0$. Since X_n has a positive probability taking negative value, we know $\{W_n\}$ will hit $\mathbb{Z}^-$ a.s. in some finite time, which implies termination. When $p > \frac{1}{2}$, by the large law of numbers, W_n a.s. tends to infinite, thus has positive probability stays positive forever ,which implies $\mathbb{P}_p(\text{percolate}) > 0$. $\square$

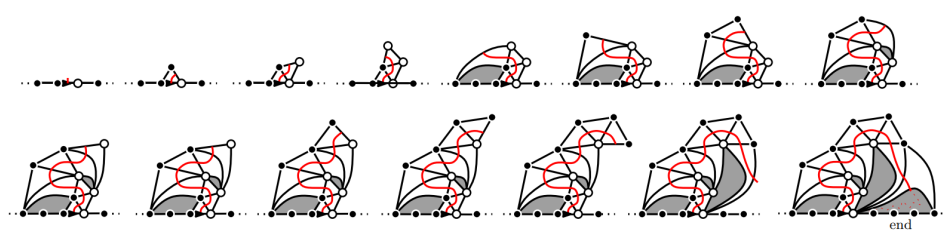

FIGURE 3.2. A complete peeling process for site percolation from [3]

Remark 3.3. We can see the peeling track is just the leftmost interface of black and white clusters. Every face in this separating line has been visited except those contained in the finite region of the last jump (see the red line in Figure 3.2).

Remark 3.4. The site percolation for quadrangulation is a bit more complicated. When we explore the interface following the algorithm above, the white vertices on the boundary need not be continuous (for example, when they are in diagonal). Richier deals with this case using a similar but more complicated method [35]. Recently, Curien and Budd have generalized these cases by **q**-Boltzmann triangulation and compute the threshold for site percolation in [11].

We continue to learn about the case with free boundary conditions. Note our case in Theorem 3.1 is somehow the "worst" boundary. Thus we can couple free boundary configuration to the fixed boundary configuration by coloring the boundary as Theorem 3.1.

Theorem 3.5. *The annealed threshold for free boundary is* $\frac{1}{2}$.

Proof. Define a projection π from the free boundary map $\mathbf{m}$ to the fixed boundary map by coloring boundary vertices of $\mathbf{m}$ to be all black except the white origin (see Figure 3.3). We can imagine the projection as conditioning on $\pi(\mathbf{m})$ (i.e. we already know the colors above the boundary).

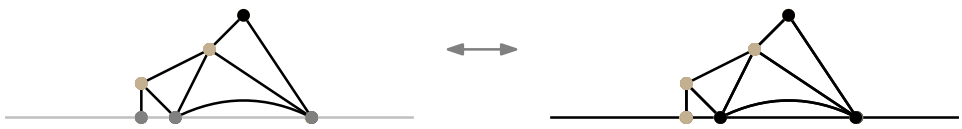

FIGURE 3.3. The coupling method. The left is the map with free boundary and the right is its projection by coloring the boundary. The grey represent the color of the vertex is unrevealed.

If the origin is in an infinite white cluster in $\pi(\mathbf{m})$, the connectivity in $\mathbf{m}$ will not be influenced by changing the color of the boundary sites except the origin (since we already have the worst case in $\pi(\mathbf{m})$), thus we will also have an infinite white cluster in $\mathbf{m}$ when the origin is white. This shows $\mathbb{P}_p(\mathbf{m}$ percolates$) > 0$, when $p > \frac{1}{2}$.

If $\pi(\mathbf{m})$ doesn't percolate, at what situation $\mathbf{m}$ will percolate? Condition on $\pi(\mathbf{m})$ doesn't percolate, following the interface exploring process defined in the proof of Theorem 3.1, we know there will be a black wall enclose the white cluster (see Figure 3.4). We call such region a stack, and the origin inside the stack is called the entrance.

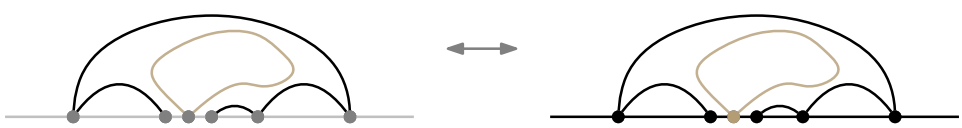

FIGURE 3.4. The left is one stack of $\mathbf{m}$, which corresponds to a bounded white cluster enclosed by a black wall (in the right).

If the white cluster can escape the stack, we only have two possible exits (the left and right endpoints in the boundary). Let A_0 denote the right exit, B_0 denote the left exit. We first reveal the color of A_0, if it is white, we grow a new stack from A_0 (note when excludes the previous stack, the boundary vertices is either black or free). There is two possible cases (see Figure 3.5), and in each situation we will still have two exits. Denote the left and the right one by B_1 and A_1 respectively. If A_0 is black, we reveal the color of B_0. If it is black, then the white cluster can not escape the stack. If it is white, we grow a new stack from B_0, then we can also get two situations similar to Figure 3.5, where there are also two exits, denoted by B_1 and A_1.

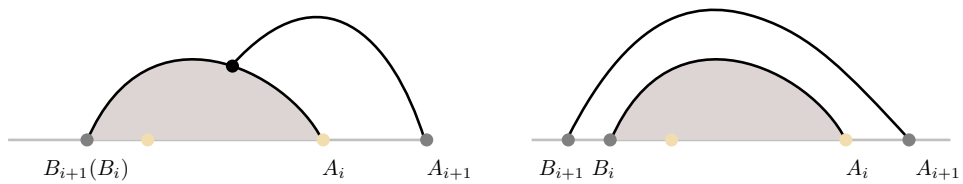

FIGURE 3.5. Two cases when growing a new stack from the old one (in brown). In every step we only have two possible exits.

We continue this process until the two exits are black, and let B_i and A_i denote the exits in step i. Thus "there is an infinite white cluster containing the root" is equivalent to "the process will never stop". Note in every step i,

$$\begin{aligned}&\mathbb{P}_p(\text{ the process will not stop at step } i \mid \pi(\mathbf{m}))\\ &\qquad = \mathbb{P}_p(\text{ at least one of the exits is white } \mid \pi(\mathbf{m})) < 1-(1-p)^2\end{aligned}$$

Since the colors of boundary vertices are independent, we have:

$$\mathbb{P}_p(\mathbf{m} \text{ percolate} \mid \pi(\mathbf{m})) \leq \lim_{n\to\infty}(p^2-2p)^n = 0$$

When $p \leq \frac{1}{2}$, $\pi(\mathbf{m})$ does not percolate a.s. Thus $\mathbf{m}$ will also do not percolate a.s. $\Rightarrow p_c = \frac{1}{2}$. □

Remark 3.6. There is another way to find the threshold by defining a peeling algorithm, which is contributed by Curien in [13]. To maintain the looking of boundary, one key idea is to keep as much randomness as we can: when we peel a triangle with a new vertex, we sometimes won't reveal its color, letting it stays free.

Proof. We first give the peeling algorithm:

Boundary condition: Free-black-free

Algorithm: We reveal the color of the boundary vertex next to the leftmost white boundary vertex. If it is white, we continue our process. If it is black, we peel from the edge immediately on the left of this vertex and continue this process until the black vertex is swallowed by these faces (i.e., there is a peeling step such that $\mathcal{R} > 1$). Recall our graph is locally finite. Thus this step is a.s. finite.

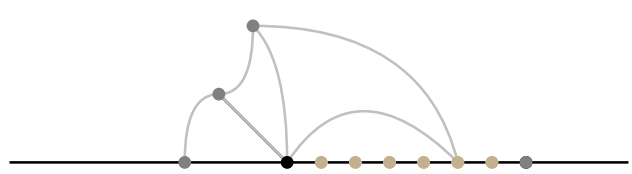

FIGURE 3.6. When a black vertex appears, we peel the adjacent faces clockwise to enclose it.

There are no straightforward terminate symbols. Even if all the white vertices have been swallowed, we still have some probability to make the cluster survive. However, we can see whenever we meet this situation, the hitting site must be white to preserve the connectivity to the infinite, which is of probability $p < 1$. Thus if

the swallow time is a.s. finite, we will meet this situation infinitely many time if percolate. Hence the annealed percolate probability goes to zero.

Now we realize the number of white boundary vertices W_n with i.i.d. increments:

$$W_n - W_{n-1} = \epsilon_n - (1-\epsilon_n)((\mathcal{R}_n \mid \mathcal{R}_n > 0) - 1)$$

where $\epsilon_n = 1$ when the color of the newly revealed vertex is white, otherwise 0. We use a condition symbol $(\mathcal{R} \mid \mathcal{R} > 0)$ to represent the series of peeling until the swallowing time. This symbol makes sense due to the spatial Markov property, as you can see every peeling is independent of previous steps. Take expectation, we have:

$$\mathbb{E}(W_n - W_{n-1}) = p - (1-p)\mathbb{E}(\mathcal{R}_n - 1 \mid \mathcal{R}_n > 0) = 2p - 1$$

Thus when $p > \frac{1}{2}$, by the law of large numbers, there is a positive probability W_n will survive forever. When $p \leq \frac{1}{2}$, W_n will a.s. hit $\mathbb{Z}^-$, and by Markov property, it will hit infinite times. Thus by our previous argument, $\mathbb{P}_p(\text{percolate}) = 0$. □

Now we turn the result to be quenched. The tool is ergodic theory or 0-1 law. Recall the shift operator θ change the root edge to the immediate left one.

Proposition 3.7. *The operator θ is mixing, hence ergodic.*

Proof. Following notation in [4], for a finite region Q which is adjacent to the boundary, we use $A_{Q,k}$ to denote the event "T contains Q, and the rightmost vertex of Q in the boundary is at a relative distance k to the left of root vertex" (k can be negative). Note that in our local metric, these $A_{Q,k}$ form a topology basis, thus we only need to prove mixing concerning these events. i.e.

$$\lim_{n\to\infty} \tau^{(\infty)}(\theta^{-n} A_{Q,k} \cap A_{Q',k'}) = \tau^{(\infty)}(A_{Q,k})\tau^{(\infty)}(A_{Q',k'})$$

Note when we take $n > |\partial Q| + |\partial Q'| + |k| + |k'|$, Q will completely be on the left side of Q' (see Figure 3.7), thus by spatial Markov property, these two events independent. Hence we have the above equation. □

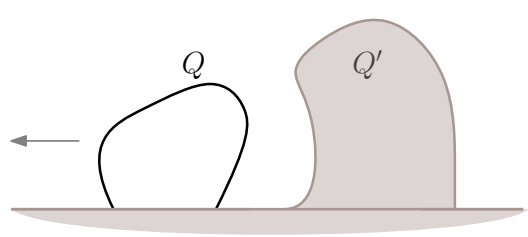

FIGURE 3.7. The two regions become disjoint when shifting enough times.

The ergodicity tells us that if one event is invariant under rerooting, the probability is 0 or 1, such as recurrence, threshold, etc. Thus as a corollary:

Theorem 3.8. *The quenched threshold for free boundary is $\frac{1}{2}$, i.e. when $p > p_c$, there is a.s. an infinite white cluster, when $p \leq p_c$, there is a.s. no infinite cluster.*

Proof. Let x_0 be the origin. When $p > p_c$, $\mathbb{P}_p($ x_0 is contained in an infinite white cluster$) > 0$. Since the event "there is an infinite white cluster which intersected the boundary" is an event invariant under the shift operator, we know $\mathbb{P}_p($ there is an infinite white cluster intersected the boundary$) = 1$.

When $p \leq p_c$, if $\mathbb{P}_p($ there is infinite cluster$) > 0$, then there is r s.t. $\mathbb{P}_p($ there is an infinite cluster intersected $B_r) > 0$. By the strong Markov property, we know it means $\mathbb{P}_p($ there is an infinite cluster intersected the boundary$) > 0$. However, we know that in each boundary point, it is a.s. not contained in an infinite white cluster when $p \leq p_c$. Thus the probability should be zero, a contradiction. □

In fact, the annealed and quenched threshold for full plane UIPT is also $\frac{1}{2}$. Since the method is similar, we leave the proof for the readers, and the details can be found in [1]. In addition, there are some other ergodic properties in UIPT, in the following two senses:

1. The shift operator θ that reroots along the simple random walk. The proof of the ergodicity is in [5]. We also use this to characterize the sequence limit of uniform measure.

2. The event invariant under local modifications around the root is 0 or 1. This is because we can use peeling to realize UIPT as an independent sequence where each random variable will carry information such as lengths, colors, etc. Thus by Kolmogorov 0-1 law, we get this proposition. For more details, see [1].

3.2. **The sub-critical regime.** Our goal in this section is to detect the "sharpness" of phase transition. In fact, when $p < p_c$, the number of white vertices on the boundary of the cluster will have a exponential decay. As for the full size of the white cluster, we can have a polynomial upper bound.

Like Section 3.1, we will first prove the proposition for the fixed boundary case (all black boundary except white origin), and then use coupling to prove the version when the boundary is free.

Proposition 3.9. *For the interface exploring peeling process in the proof of Theorem 3.1, let W_n be the number of white vertices along the boundary in step n. Then there exists $\theta > 0$, s.t. for any constant $c \geq 0$, $\mathbb{P}_p(W_n \geq c+1) \leq e^{-c-n\theta}$.*

Proof. Let $X_i := W_{i+1} - W_i$, which are i.i.d. increments before the stopping time. $W_0 = 1$. Then $\mathbb{E}e^{t(W_n-1)} = (\mathbb{E}e^{tX_1})^n$. We first show there exists $t > 0$, s.t. $\mathbb{E}e^{tX_1} < 1$. Let q_k $(k = -1, 1, 2, 3 \dots)$ be the probability defined in Proposition 2.18. Recall the possible values of X_1 in Proposition 3.1, we get:

$$\mathbb{E}e^{tX_1} = pq_{-1}e^t + (1-p)q_{-1} + \sum_{k=1}^{\infty} q_k e^{-kt} + \sum_{k=1}^{\infty} q_k := f(t)$$

$$f'(0) = pq_{-1} - \sum_{k=1}^{\infty} kq_k = p(\mathbb{E}\mathcal{E} - 1) - \mathbb{E}\mathcal{R} \overset{(2.12)}{=} \delta(p - \frac{1}{2}) < 0$$

Thus there exist $t > 0$, $f(t) < f(0) = 1$. Let $\theta = -\log f(t)$. Since for any $c \geq 0$, $W_n \geq c+1$ implies n is before the stopping time, we have:

$$\mathbb{P}_p(W_n - 1 \geq c) \leq e^{-c}(\mathbb{E}e^{t(W_n-1)}) = e^{-tc}(\mathbb{E}e^{tX_1})^n \leq e^{-c-n\theta}.$$

□

We will have $W_n \geq 1$ when $n <$ the stopping time $\mathcal{N}^-$. Take $c = 1$, we have corollary:

Proposition 3.10. *When $p < p_c$, the stopping time $\mathcal{N}^-$ will have a exponential decay, i.e.*

$$\exists\ \theta > 0,\ \mathbb{P}_p(\mathcal{N}^- > n) \leq e^{-n\theta}.$$

Remark 3.11. When $p = p_c$, we will not have a exponential decay, but with a polynomial tail. The proof is based on functional CLT of W_n in the critical phase (here we will not terminate it in the stopping time $\mathcal{N}^-$) [8]:

$$\left(\frac{W_{\lfloor nt \rfloor}}{n^{2/3}}\right)_{t\geq 0} \xrightarrow[n\to\infty]{(d)} \kappa \cdot (\mathcal{S}_t)_{t\geq 0}$$

where $(\mathcal{S}_t)_{t\geq 0}$ is a $\frac{3}{2}$-stable process with no positive jump, κ is a universal constant, and the convergence is about Skorokhod topology. Then let $\mathcal{N}^- = \inf\{i \mid W_i \leq 0\}$, we will have $\mathbb{P}(\mathcal{N}^- = n) \sim c \cdot n^{-4/3}$ by analysis of the stable process in [14, Theorem 1].

To estimate the size of the white cluster, we define the hull $\mathcal{H}$ of the white cluster which is the white cluster along with the vertices in the finite holes it encloses. Following the interface exploration process defined in Theorem 3.1, we denote the number of vertices added into $\mathcal{H}$ in the i-th step by Y_i. Thus

$$Y_i \text{ follows Bernoulli}(p), \text{ when } \mathcal{E}_i = 2$$
$$Y_i \text{ follows Boltzmann } \mu_k, \text{ when } \mathcal{R}_i = k-1$$

Proposition 3.12. *When $p < p_c$, $|\mathcal{H}|$ will have a polynomial decay. i.e.*

$$\exists\ \theta > 0,\ \mathbb{P}_p(|\mathcal{H}| \geq n) \leq n^{-\theta} \text{ when } p < p_c.$$

Remark 3.13. We will not have a exponential decay for the hull. Since the moment generating function

$$\mathbb{E}[\exp(\theta X_1)] \geq q_1 \sum \frac{\varphi_{t,2}}{Z_2(\alpha^{-1})} \alpha^{-t} e^{\theta t} = q_1 \frac{Z_2(\alpha^{\epsilon-1})}{Z_2(\alpha^{-1})} = \infty, \forall \theta > 0$$

where $\alpha^\epsilon = e^\theta > 1$, $\epsilon > 0$, $Z_m(t) := \sum_{n=0}^\infty \varphi_{n,m} t^n$. However, we still expect a exponential decay for the cluster size.

Lemma 3.14 ([1])**.** $\mathbb{E}[Y_i \mid R_i = k] \sim \frac{2}{3}k^2$.

The lemma is proved by computing the derivative of $Z_k(t)$, and we omit the details here. The Jensen equality tells us $\mathbb{E}[Y_i^\theta | \mathcal{R}_i] \leq (\mathbb{E}[Y_i | \mathcal{R}_i])^\theta$, for any $0 < \theta < 1$. Thus as corollary:

Lemma 3.15. *For any $0 < \theta < 2$ there exists $0 < \theta_1 < 1$, $\mathbb{E}[Y_i^{\theta_1} | \mathcal{R}_i] \leq (\mathcal{R}_i)^\theta$.*

Another important asymptotics for q_k is:

Lemma 3.16. *$q_k \sim ck^{-5/2}$, as $k \to \infty$.*

Proof. Recall (2.10) we have $q_k = Z_{k+1}\beta^{-k}$. By a reparametrization appearing in [1, Proposition 1.7] and [18], we have

$$Z_{k+1} = \beta^{-k}\left(\frac{(2(k-1))!}{(k-1)!(k+1)!}\beta^k\right) \sim ck^{-5/2}$$

where c is some constant > 0, and the asymptotics comes from the Stirling formula. □

Proof of Proposition 3.12. Take $\theta = 1$ in Lemma 3.15, then $\exists\, 0 < \theta_1 < 1$, $\mathbb{E}[Y_i^{\theta_1}|\mathcal{R}_i] \leq \mathcal{R}_i$, thus

$$\mathbb{E}[Y_i^{\theta_1}] = q_{-1}p + \sum_{k=1}^{\infty} q_k \mathbb{E}[Y_i^{\theta_1}|\mathcal{R}_i = k] \lesssim q_{-1}p + \sum_{k=1}^{\infty} k^{-5/2+1} < \infty$$

The size of the hull $|\mathcal{H}| \leq 1 + Y_1 + \cdots + Y_{\mathcal{N}^-}$, where N^- is the stopping time. Recall for any $0 < t < 1$, we have $(x+y)^t \leq x^t + y^t$ for $x, y \geq 0$, thus

$$\mathbb{E}|\mathcal{H}|^{\theta_1/2} \leq 1 + \mathbb{E}(Y_1^{\theta_1/2} + \cdots + Y_{\mathcal{N}^-}^{\theta_1/2}) = 1 + \sum_{i=1}^{\infty} \mathbb{E} Y_i^{\theta_1/2} 1_{\mathcal{N}^- \geq i}$$

Apply Cauchy inequality:

$$\mathbb{E}|\mathcal{H}|^{\theta_1/2} \leq 1 + \sum_{i=1}^{\infty} (\mathbb{E} Y_i^{\theta_1})^{1/2} \mathbb{P}_p(\mathcal{N}^- \geq i)^{1/2} \lesssim 1 + \sum_{i=1}^{\infty} \mathbb{P}_p(\mathcal{N}^- \geq i)^{1/2} < \infty$$

The last inequality comes form Proposition 3.10. Then by Chebyshev inequality,

$$\mathbb{P}_p(|\mathcal{H}| \geq n) \leq n^{-\theta_1/2} \mathbb{E}|\mathcal{H}|^{\theta_1/2} \leq n^{-\theta_0}, \text{ for some } \theta_0 > 0$$

□

Remark 3.17. The estimates here is rough. For a precise exponents at $p = p_c$, $\mathbb{P}_p(|\mathcal{H}| > n) = n^{-1/4+o(1)}$, which can be found in [3, §4.2]. The exponents is important due to a physics prediction called KPZ relation [23], which states a relationship between the critical exponents on a regular lattice and on a random lattice. It has been checked for many objects in the past decades.

We continue to learn about the case with free boundary conditions. By the coupling in the proof of Theorem 3.5, we know the size of the white cluster is almostly controlled by the size of the hull of these stacks. Let $\mathcal{C}$ be the white cluster of the origin, we have:

Proposition 3.18. *When $p < p_c$, $|\mathcal{C}|$ will have a polynomial decay. i.e.*

$$\exists\ \theta > 0,\ \mathbb{P}_p(|\mathcal{C}| \geq n) \leq n^{-\theta}.$$

Proof. We first show that in one stack, $|\mathcal{C}|$ will have a polynomial decay. Using Proposition 3.12, we know the part of the hull inside the black wall (see the yellow region in Figure 3.8) will have a polynomial decay. However, when the track forms a hole that is adjacent to the boundary of the half-plane, the vertices in these holes could be connected to the hull (since we can have the color of the hitting point to be white). See these holes in the blue region in Figure 3.8. Fortunately, we will only have at most $\mathcal{N}^-$ many these holes. Thus similar as estimates for $\mathcal{H}$ in Proposition 3.12, there is $0 < \theta < 1$, the θ-moment of the total size is finite. As for the vertices in boundary of these holes, we have $\sum_{k=1} q_k k^\theta \lesssim \sum_{k=1} k^{-3/2} < \infty$. Hence the θ-moment of the number of vertices in $\{\ \mathcal{C} \cap \text{the stack}\}$ is finite.

We already know in the proof of Proposition 3.1 that the size of these holes will have a polynomial decay. Thus since $\mathcal{N}^-$ has a exponential decay, we have the polynomial decay of the sum of these holes, which implies a polynomial decay of $|\mathcal{C}|$ in one stack.

Let N be the number of stacks that intersects $\mathcal{C}$, and $\mathcal{C}_1 \ldots \mathcal{C}_N$ be the parts of $\mathcal{C}$ in these stacks. If $N \geq 2^n$, we will have one white path that intersects at least n stacks (since every stack only have two exits). The color of the entrance of these

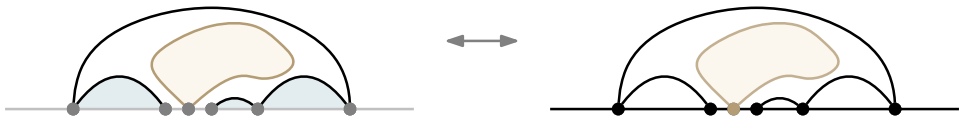

FIGURE 3.8. The hull in one stack. The creamy regions are the original hull. The blue regions are possible vertices that can be added into the hole when changing the color of the boundary.

stacks have to be white and they are independent. Thus $\mathbb{P}_p(N \geq 2^n) \leq p^n$. Since $p < 1/2$, there is $c > 1$, $\mathbb{P}_p(N \geq n) \lesssim n^{-c}$. Recall for any $0 < t < 1$, we have $(x+y)^t \leq x^t + y^t, \forall\, x, y \geq 0$, we then get

$$\mathbb{E}|\mathcal{C}|^{t\theta} \leq \mathbb{E}\left(|\mathcal{C}_1|^{t\theta} + \ldots |\mathcal{C}_N|^{t\theta}\right) = \sum_{n=1}^{\infty} \mathbb{E}|\mathcal{C}_n|^{t\theta} 1_{N \geq n}$$

Select $0 < t < 1$ s.t. $(1-t)c > 1$, then apply Hölder equality,

$$\mathbb{E}|\mathcal{C}|^{t\theta} \leq \sum_{n=1}^{\infty} (\mathbb{E}|\mathcal{C}_n|^{\theta})^t (\mathbb{P}_p(N \geq n))^{1-t} \lesssim \sum_{n=1}^{\infty} \mathbb{P}_p(N \geq n)^{1-t} \lesssim \sum_{n=1}^{\infty} n^{-(1-t)c} < \infty$$

Thus by Chebyshev inequality we have a polynomial decay of $|\mathcal{C}|$. □

3.3. **The number of infinite clusters.** When $p > p_c$, there will be an infinite cluster, and a natural question is raised: How about the number of the infinite clusters? Intuition from the Burton-Keane theorem [12] in deterministic lattice percolation tells us there should be a unique infinite cluster for almost all T. We will prove this for UIHPT. The proof for UIPT is similar.

The key idea is considering the crossing events. For any simply connected region $\mathcal{D}$ enclosed by vertices $ABCD$ on $\partial\mathbf{M}$ and a simple path inside $\mathbf{M}$ form A to D, we use $\curvearrowleft_w \mathcal{D}$ if there is a horizontal white path connecting AB and CD. We use $\updownarrow_b \mathcal{D}$ if a vertical black path connects AD and BC. (See Figure 3.9)

FIGURE 3.9. Crossing events

Lemma 3.19. *Exactly one of* $\updownarrow_b \mathcal{D}$ *and* $\curvearrowleft_w \mathcal{D}$ *happens.*

Proof. **Case1** : If A is black, we explore along $A \to B$ until we find some white vertex, then start peeling from this edge, with a white vertex in the left and black on the right; If we can't find a white point, we get the event $\updownarrow_b \mathcal{D}$.

Case2 : If A is white, we explore along $A \to D$ until we find some white vertex, then start peeling from this edge, with a white vertex in the left and black on the right; If we can't find a black point, we get the event $\curvearrowleft_w \mathcal{D}$.

The process will stop when hitting $\partial\mathcal{D}$ at a point with the same color as the outer boundary of the revealed part. When hitting AB, we can regard the hitting point A' as A, and come back to case 1. Note if A' has a black path to CB, A can

also have a black path to CB (see Figure 3.10. In the following figures, we will use the white (creamy) line to stand for a white path, black line for a black path. The edges we start peeling are in red. The blue region are the parts we excludes when reset A' as A.)

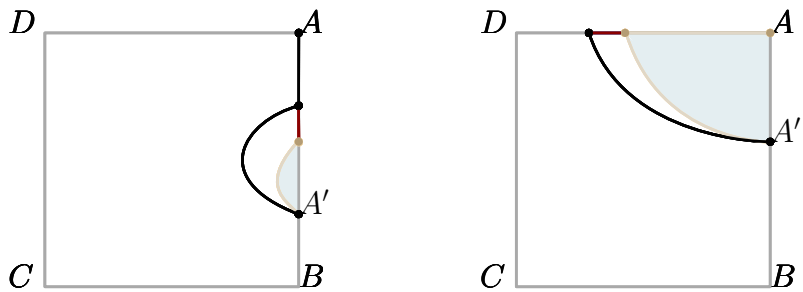

FIGURE 3.10. Stop at AB. Left is starting case 1, right is case 2.

Similarly, when hitting AD, we can regard the hitting point A' as A, and come back to case 2. (see Figure 3.11)

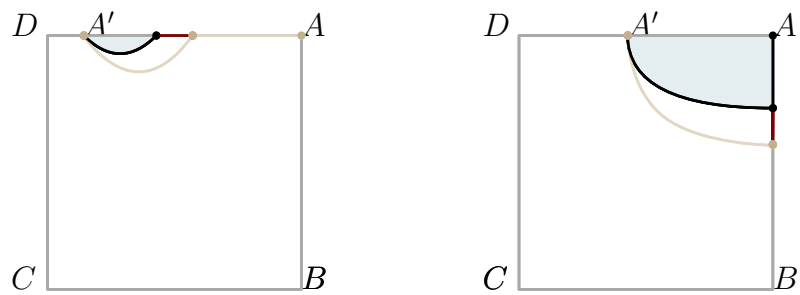

FIGURE 3.11. Stop at AD. Left is starting case 2, right is case 1.

If it hits DC at a white point, we find a white path from AB to DC. If black, then we can regard hitting point D' as D, and continue peeling from the adjacent edge in the left side of the interface (see Figure 3.12). If it hits BC, the process is the same. (see Figure 3.13)

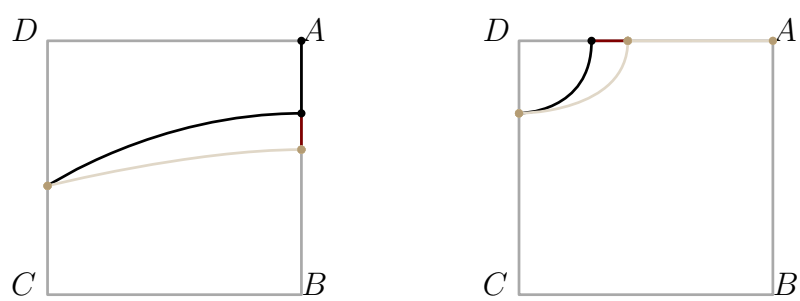

FIGURE 3.12. Stop at DC. Left is starting case 1, right is case 2.

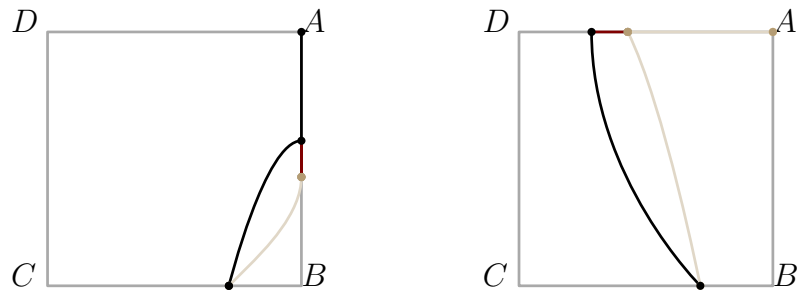

FIGURE 3.13. Stop at BC. Left is starting case 1, right is case 2.

Since $\mathcal{D}$ has finite vertices, the process will terminate in finite steps. Thus we can get either $\curvearrowleft_w \mathcal{D}$ or $\updownarrow_b \mathcal{D}$ (these two events can't happen simultaneously). □

Our next goal is to control $\mathbb{P}_p(\updownarrow_b \mathcal{D})$ in semi-annuli, where the lemma can be applied due to the spatial Markov property.

Proposition 3.20. *When $p < p_c$, there is a constant $\theta > 0$, $\mathbb{P}(x \leftrightarrow \partial B(x,n)) \leq n^{-\theta}$, where x is the origin.*

Proof. If there is a white path from the origin to $\partial B(x,n)$, the size of the white cluster $|\mathcal{C}|$ that contains the origin is at least n. Then apply Proposition 3.18. □

Let $\mathcal{D}_n$ be the semi-annulus enclosed by $\partial \bar{B}_{r_n}$ and $\partial \bar{B}_{r_{n+1}}$. Here, $\bar{B}_n$ is the n-ball formed during the metric peeling process (see the arguments below Theorem 2.17). It is simply connected and with every point in the outer boundary at distance ≥ 1 from $\partial \bar{B}_{n-1}$. We define the random length r_n by induction: $r_1 = 1$; $r_{n+1} = r_n + \lceil (n^2 l_n)^{1/\theta} \rceil$, where l_n is the perimeter of $\partial \bar{B}_{r_n}$.

Proposition 3.21. $\mathbb{P}(\updownarrow_b \mathcal{D}_n) \lesssim n^{-2}$, *as $n \to \infty$.*

Proof. Let $\partial \bar{B}_{r_n}$ with vertices $x_1, ..., x_{l_n}$. By the invariance of re-rooting along $\partial \mathbf{M}$, proposition 3.20 applies for each x_i. Since $p_c = 1/2$, changing the color in Lemma 3.20, we get:

$$\begin{aligned}
\mathbb{P}(\updownarrow_b \mathcal{D}_n) &\leq \mathbb{E} \sum\nolimits_{i=1}^{l_n} \mathbb{P}_p(\updownarrow_b \mathcal{D}_n, \text{ start at } x_i) \\
&\leq \mathbb{E} \sum\nolimits_{i=1}^{l_n} \mathbb{P}_p(x_i \leftrightarrow \partial B(x_i, r_{n+1} - r_n)) \\
&\leq \mathbb{E} l_n (r_{n+1} - r_n)^{-\theta} \leq n^{-2}
\end{aligned}$$

□

Theorem 3.22. *In site percolation on UIHPT with free boundary condition, let k_p denote the number of infinite clusters. Then $k_p = 0$ a.s. for $p \leq \frac{1}{2}$; $k_p = 1$ a.s. for $p > \frac{1}{2}$.*

Proof. We have proved the sub-critical case in Theorem 3.8. When $p > p_c$, if $\mathbb{P}_p(k_p \geq 2) > 0$, then there is N, $\mathbb{P}_p(\text{at least 2 infinite clusters cross } \mathcal{D}_N) > 0$. Thus for all $n \geq N$, the probabilities are also positive. By the lemmas above, we have $\sum \mathbb{P}_p(\updownarrow_b \mathcal{D}_n) \leq \sum n^{-2} < \infty$. Thus by Borel-Cantelli, $\updownarrow_b \mathcal{D}_n$ will a.s. happen finitely many times. Then by Lemma 3.19, $\curvearrowleft_w \mathcal{D}_n$ will happen for all but finite

many times. However, whenever two infinite white clusters cross such $\mathcal{D}_n$, they will be connected if $\curvearrowleft_w D_n$ occurs. Thus we get a contradiction. □

Remark 3.23. We could also use the above method to prove the uniqueness of infinite cluster in UIPT. First we consider the crossing event. However, Lemma 3.19 cannot be applied directly to UIPT, since the rings is not simply connected. But in super-critical regime we will a.s. have a simple white path to the infinite, then we can cut the ring by the segment of this path to get a simply connected region. Next, study the polynomial decay of the probability of $x \leftrightarrow \partial B(x, n)$ by similar method in Section 3.2. Finally, use similar argument in Theorem 3.22, we get our conclusion.

Remark 3.24. Curien gives another proof in [13, §11], where he proves the case for face percolation and leaves the proof for site to the readers. The method is considering the interface with black in the left and white in the right, when condition on the boundary intersects two infinite white cluster with distance k along the boundary. The interface will a.s. hits the boundary at distance $> k$ from the starting point. If hits the right side, the right white cluster will be finite; if hits the left side, the two white cluster will be connected. Hence we get a contradiction.

Curien's proof will not rely on p_c and is more general. However, in our proof we can get some by-products and yield a quantitative information. For example, for a finite region $\mathcal{D}$, we can get an upper bound for the probability that there are two cluster which intersect $\mathcal{D}$ but do not meet inside $\mathcal{D}$.

Acknowledgements

First and foremost, I would like to extend my sincere gratitude to my advisor Ewain Gwynne, for agreeing to mentor me in the summer research; for proposing the research topic and suggesting reading materials; for the inspiring and helpful discussions; for the patient and elaborative comments on my draft; for arousing my interests on random geometry and encouraging me to the further study on probability. He set up a role model of a mathematician, and the good habits I obtained from his instruction will definitely benefit me for the whole time of life.

Special thanks to Peter May for organizing the REU project and Liang Xiao for recommending me to attend. I'm also grateful to Gregory Lawler and other members in the probability group of the University of Chicago for their instructive lectures.

I could not leave out my gratitude to my friends at Peking University, who give me suggestions and share my feelings in the period from applying the project to finishing this paper. To mention but a few of them: Xinyi Li, Zijie Zhuang, Jiayue Chen, Yufan Chen, Xiangtao Chen, and other members in Xinyi's probability seminar.

I would also like to thank dozens of stray cats on the campus for their companionship on many lonely nights and the fun they brought to me, especially Yolk, Shampoo, and Orange.

And finally my family: Mum and Dad for the always support, my cats Weiwei and Xinxin for their mercy on my keyboard.

References

[1] Omer Angel. "Growth and percolation on the uniform infinite planar triangulation". In: *Geom. Funct. Anal.* 13.5 (2003), pp. 935–974. ISSN: 1016-443X. DOI: 10.1007/s00039-003-0436-5. URL: https://doi.org/10.1007/s00039-003-0436-5.

[2] Omer Angel. "Scaling of Percolation on Infinite Planar Maps, I". In: *arXiv Mathematics e-prints*, math/0501006 (Dec. 2004), math/0501006. arXiv: math/0501006 [math.PR].

[3] Omer Angel and Nicolas Curien. "Percolations on random maps I: Half-plane models". In: *Ann. Inst. Henri Poincaré Probab. Stat.* 51.2 (2015), pp. 405–431. ISSN: 0246-0203. DOI: 10.1214/13-AIHP583. URL: https://doi.org/10.1214/13-AIHP583.

[4] Omer Angel and Gourab Ray. "Classification of half-planar maps". In: *Ann. Probab.* 43.3 (2015), pp. 1315–1349. ISSN: 0091-1798. DOI: 10.1214/13-AOP891. URL: https://doi.org/10.1214/13-AOP891.

[5] Omer Angel and Oded Schramm. "Uniform infinite planar triangulations". In: *Comm. Math. Phys.* 241.2-3 (2003), pp. 191–213. ISSN: 0010-3616. DOI: 10.1007/978-1-4419-9675-6_16. URL: https://doi.org/10.1007/978-1-4419-9675-6_16.

[6] Itai Benjamini and Oded Schramm. "Recurrence of distributional limits of finite planar graphs". In: *Electron. J. Probab.* 6 (2001), no. 23, 13. ISSN: 1083-6489. DOI: 10.1214/EJP.v6-96. URL: https://doi.org/10.1214/EJP.v6-96.

[7] Nathanaël Berestycki and Ellen Powell. *Gaussian free field, Liouville quantum gravity and Gaussian multiplicative chaos*. https://www.ams.org/open-math-notes/omn-view-listing?listingId=111291. 2021.

[8] Jean Bertoin. *Random fragmentation and coagulation processes*. Vol. 102. Cambridge Studies in Advanced Mathematics. Cambridge University Press, 2006, pp. viii+280. ISBN: 978-0-521-86728-3; 0-521-86728-2. DOI: 10.1017/CBO9780511617768. URL: https://doi.org/10.1017/CBO9780511617768.

[9] Jean Bertoin, Nicolas Curien, and Igor Kortchemski. "Random planar maps and growth-fragmentations". In: *Ann. Probab.* 46.1 (2018), pp. 207–260. ISSN: 0091-1798. DOI: 10.1214/17-AOP1183. URL: https://doi.org/10.1214/17-AOP1183.

[10] Timothy Budd. "The peeling process of infinite Boltzmann planar maps". In: *Electron. J. Combin.* 23.1 (2016), Paper 1.28, 37.

[11] Timothy Budd and Nicolas Curien. "Simple peeling of planar maps with application to site percolation". In: *arXiv e-prints*, arXiv:1909.10217 (Sept. 2019), arXiv:1909.10217. arXiv: 1909.10217 [math.PR].

[12] R. M. Burton and M. Keane. "Density and uniqueness in percolation". In: *Comm. Math. Phys.* 121.3 (1989), pp. 501–505. ISSN: 0010-3616. URL: http://projecteuclid.org/euclid.cmp/1104178143.

[13] Nicolas Curien. *Peeling random maps*. https://www.imo.universite-paris-saclay.fr/~curien/enseignement.html. 2020.

[14] R. A. Doney. "On the exact asymptotic behaviour of the distribution of ladder epochs". In: *Stochastic Process. Appl.* 12.2 (1982), pp. 203–214. ISSN: 0304-4149. DOI: 10.1016/0304-4149(82)90042-4. URL: https://doi.org/10.1016/0304-4149(82)90042-4.

[15] Bertrand Duplantier, Jason Miller, and Scott Sheffield. "Liouville quantum gravity as a mating of trees". In: *arXiv e-prints*, arXiv:1409.7055 (Sept. 2014), arXiv:1409.7055. arXiv: 1409.7055 [math.PR].

[16] Bertrand Duplantier and Scott Sheffield. "Liouville quantum gravity and KPZ". In: *Invent. Math.* 185.2 (2011), pp. 333–393. ISSN: 0020-9910. DOI: 10.1007/s00222-010-0308-1. URL: https://doi.org/10.1007/s00222-010-0308-1.

[17] Rick Durrett. *Probability—theory and examples*. Vol. 49. Cambridge Series in Statistical and Probabilistic Mathematics. Fifth edition of [MR1068527]. Cambridge University Press, Cambridge, 2019, pp. xii+419. ISBN: 978-1-108-47368-2. DOI: 10.1017/9781108591034. URL: https://doi.org/10.1017/9781108591034.

[18] Ian P. Goulden and David M. Jackson. *Combinatorial enumeration*. With a foreword by Gian-Carlo Rota, Reprint of the 1983 original. Dover Publications, Inc., Mineola, NY, 2004, pp. xxvi+569. ISBN: 0-486-43597-0.

[19] Ewain Gwynne. "Random surfaces and Liouville quantum gravity". In: *Notices Amer. Math. Soc.* 67.4 (2020), pp. 484–491. ISSN: 0002-9920. DOI: 10.1090/noti. URL: https://doi.org/10.1090/noti.

[20] Ewain Gwynne and Jason Miller. "Convergence of percolation on uniform quadrangulations with boundary to SLE_6 on $\sqrt{8/3}$-Liouville quantum gravity". In: *arXiv e-prints*, arXiv:1701.05175 (Jan. 2017), arXiv:1701.05175. arXiv: 1701.05175 [math.PR].

[21] Nina Holden and Xin Sun. "Convergence of uniform triangulations under the Cardy embedding". In: *arXiv e-prints*, arXiv:1905.13207 (May 2019), arXiv:1905.13207. arXiv: 1905.13207 [math.PR].

[22] V. A. Kazakov. "Percolation on a fractal with the statistics of planar Feynman graphs: exact solution". In: *Modern Phys. Lett. A* 4.17 (1989), pp. 1691–1704. ISSN: 0217-7323. DOI: 10.1142/S0217732389001921. URL: https://doi.org/10.1142/S0217732389001921.

[23] V. G. Knizhnik, A. Polyakov, and A. Zamolodchikov. "Fractal Structure of 2D Quantum Gravity". In: *Modern Physics Letters A* 03 (1988), pp. 819–826.

[24] M. A. Krikun. "A uniformly distributed infinite planar triangulation and a related branching process". In: *Zap. Nauchn. Sem. S.-Peterburg. Otdel. Mat. Inst. Steklov. (POMI)* 307.Teor. Predst. Din. Sist. Komb. i Algoritm. Metody. 10 (2004), pp. 141–174, 282–283. ISSN: 0373-2703. DOI: 10.1007/s10958-005-0424-4. URL: https://doi.org/10.1007/s10958-005-0424-4.

[25] Robert Langlands, Philippe Pouliot, and Yvan Saint-Aubin. "Conformal invariance in two-dimensional percolation". In: *Bull. Amer. Math. Soc. (N.S.)* 30.1 (1994), pp. 1–61. ISSN: 0273-0979. DOI: 10.1090/S0273-0979-1994-00456-2. URL: https://doi.org/10.1090/S0273-0979-1994-00456-2.

[26] Gregory F. Lawler, Oded Schramm, and Wendelin Werner. "Values of Brownian intersection exponents. I. Half-plane exponents". In: *Acta Math.* 187.2 (2001), pp. 237–273. ISSN: 0001-5962. DOI: 10.1007/BF02392618. URL: https://doi.org/10.1007/BF02392618.

[27] Jean-François Le Gall. "Uniqueness and universality of the Brownian map". In: *Ann. Probab.* 41.4 (2013), pp. 2880–2960. ISSN: 0091-1798. DOI: 10.1214/12-AOP792. URL: https://doi.org/10.1214/12-AOP792.

[28] Jean-François Le Gall and Grégory Miermont. "Scaling limits of random trees and planar maps". In: *Probability and statistical physics in two and more dimensions*. Vol. 15. Clay Math. Proc. Amer. Math. Soc., Providence, RI, 2012, pp. 155–211.

[29] Russell Lyons and Yuval Peres. *Probability on trees and networks*. Vol. 42. Cambridge Series in Statistical and Probabilistic Mathematics. Cambridge University Press, New York, 2016, pp. xv+699. ISBN: 978-1-107-16015-6. DOI: 10.1017/9781316672815. URL: https://doi.org/10.1017/9781316672815.

[30] Grégory Miermont. "The Brownian map is the scaling limit of uniform random plane quadrangulations". In: *Acta Math.* 210.2 (2013), pp. 319–401. ISSN: 0001-5962. DOI: 10.1007/s11511-013-0096-8. URL: https://doi.org/10.1007/s11511-013-0096-8.

[31] Jason Miller and Scott Sheffield. "An axiomatic characterization of the Brownian map". In: *J. Éc. polytech. Math.* 8 (2021), pp. 609–731. ISSN: 2429-7100. DOI: 10.5802/jep.15. URL: https://doi.org/10.5802/jep.15.

[32] Jason Miller and Scott Sheffield. "Liouville quantum gravity and the Brownian map I: the QLE$(8/3, 0)$ metric". In: *Invent. Math.* 219.1 (2020), pp. 75–152. ISSN: 0020-9910. DOI: 10.1007/s00222-019-00905-1. URL: https://doi.org/10.1007/s00222-019-00905-1.

[33] A. M. Polyakov. "Quantum geometry of fermionic strings". In: *Phys. Lett. B* 103.3 (1981), pp. 211–213. ISSN: 0370-2693. DOI: 10.1016/0370-2693(81)90744-9. URL: https://doi.org/10.1016/0370-2693(81)90744-9.

[34] Rémi Rhodes and Vincent Vargas. "KPZ formula for log-infinitely divisible multifractal random measures". In: *ESAIM Probab. Stat.* 15 (2011), pp. 358–371. ISSN: 1292-8100. DOI: 10.1051/ps/2010007. URL: https://doi.org/10.1051/ps/2010007.

[35] Loïc Richier. "Universal aspects of critical percolation on random half-planar maps". In: *Electron. J. Probab.* 20 (2015), Paper No. 129, 45. DOI: 10.1214/EJP.v20-4041. URL: https://doi.org/10.1214/EJP.v20-4041.

[36] Oded Schramm. "Scaling limits of loop-erased random walks and uniform spanning trees". In: *Israel J. Math.* 118 (2000), pp. 221–288. ISSN: 0021-2172. DOI: 10.1007/BF02803524. URL: https://doi.org/10.1007/BF02803524.

[37] Scott Sheffield. "Conformal weldings of random surfaces: SLE and the quantum gravity zipper". In: *Ann. Probab.* 44.5 (2016), pp. 3474–3545. ISSN: 0091-1798. DOI: 10.1214/15-AOP1055. URL: https://doi.org/10.1214/15-AOP1055.

[38] Stanislav Smirnov. "Critical percolation in the plane: conformal invariance, Cardy's formula, scaling limits". In: *C. R. Acad. Sci. Paris Sér. I Math.* 333.3 (2001), pp. 239–244. ISSN: 0764-4442. DOI: 10.1016/S0764-4442(01)01991-7. URL: https://doi.org/10.1016/S0764-4442(01)01991-7.

[39] W. T. Tutte. "A census of Hamiltonian polygons". In: *Canadian J. Math.* 14 (1962), pp. 402–417. ISSN: 0008-414X. DOI: 10.4153/CJM-1962-032-x. URL: https://doi.org/10.4153/CJM-1962-032-x.

[40] W. T. Tutte. "A census of planar maps". In: *Canadian J. Math.* 15 (1963), pp. 249–271. ISSN: 0008-414X. DOI: 10.4153/CJM-1963-029-x. URL: https://doi.org/10.4153/CJM-1963-029-x.

[41] W. T. Tutte. "A census of planar triangulations". In: *Canadian J. Math.* 14 (1962), pp. 21–38. ISSN: 0008-414X. DOI: 10.4153/CJM-1962-002-9. URL: https://doi.org/10.4153/CJM-1962-002-9.

[42] W. T. Tutte. "A census of slicings". In: *Canadian J. Math.* 14 (1962), pp. 708–722. ISSN: 0008-414X. DOI: 10.4153/CJM-1962-061-1. URL: https://doi.org/10.4153/CJM-1962-061-1.

[43] Yoshiyuki Watabiki. "Construction of non-critical string field theory by transfer matrix formalism in dynamical triangulation". In: *Nuclear Phys. B* 441.1-2 (1995), pp. 119–163. ISSN: 0550-3213. DOI: 10.1016/0550-3213(95)00010-P. URL: https://doi.org/10.1016/0550-3213(95)00010-P.

[44] Ariel Yadin. *An introduction to percolation*. https://www.math.bgu.ac.il/~yadina/percolation.pdf. 2020.